Cell. Mol. Life Sci. (2017) 74:2095–2106
DOI 10.1007/s00018-017-2456-6

Cellular and Molecular Life Sciences

ORIGINAL ARTICLE

Defective germinal center B-cell response and reduced arthritic pathology in microRNA-29a-deficient mice

Annemarie van Nieuwenhuijze[1,2] · James Dooley[1,2] · Stéphanie Humblet-Baron[1,2] · Jayasree Sreenivasan[1,2] · Marije Koenders[3] · Susan M. Schlenner[1,2] · Michelle Linterman[4] · Adrian Liston[1,2]

Received: 21 June 2016 / Revised: 14 December 2016 / Accepted: 3 January 2017 / Published online: 25 January 2017

Abstract MicroRNA (miR) are short non-coding RNA sequences of 19–24 nucleotides that regulate gene expression by binding to mRNA target sequences. The *miR-29* family of miR (*miR-29a, b-1, b-2* and *c*) is a key player in T-cell differentiation and effector function, with deficiency causing thymic involution and a more inflammatory T-cell profile. However, the relative roles of different *miR-29* family members in these processes have not been dissected. We studied the immunological role of the individual members of the *miR-29* family using mice deficient for *miR-29a/b-1* or *miR-29b-2/c* in homeostasis and during collagen-induced arthritis. We found a definitive hierarchy of immunological function, with the strong phenotype of *miR-29a*-deficiency in thymic involution and T-cell activation being reduced or absent in *miR-29c*-deficient mice. Strikingly, despite elevating the Th1 and Th17 responses, loss of *miR-29a* conferred near-complete protection from collagen-induced arthritis (CIA), with profound defects in B-cell proliferation and antibody production. Our results identify the hierarchical structure of the *miR-29* family in T-cell biology, and identify *miR-29a* in B cells as a potential therapeutic target in arthritis.

Keywords MicroRNA · Thymic involution · Experimental arthritis · Autoimmune pathology

Abbreviations

CIA	Collagen-induced arthritis
CII	Type II collagen
CFA	Complete Freund's adjuvant
DC	Dendritic cell
GC	Germinal center
Het	Heterozygous
HRP	Horseradish peroxidase
H&E	Haematoxylin and eosin
IFN	Interferon
IL	Interleukin
KO	Knockout
miR	MicroRNA
PG	Proteoglycan
PMA	Phorbol myristate acetate
RF	Rheumatoid factor
SafO	Safranin O
SRBC	Sheep red blood cells
Teff	Effector T cell
Th	T helper cell
Tfh	T follicular helper cell
Tfr	T follicular regulatory cell
Tn	Naïve T cell
Treg	Regulatory T cell
WT	Wildtype

A. van Nieuwenhuijze and J. Dooley contributed equally.

✉ Adrian Liston
adrian.liston@vib.be

[1] VIB Center for Brain and Disease Research, VIB, KU Leuven Campus Gasthuisberg, Herestraat 49, bus 1026, 3000 Leuven, Belgium

[2] Department of Microbiology and Immunology, University of Leuven, Leuven, Belgium

[3] Experimental Rheumatology, Radboud University Medical Center, 6525 Nijmegen, GA, The Netherlands

[4] Laboratory of Lymphocyte Signaling and Development, Babraham Institute, Cambridge CB22 3AT, UK

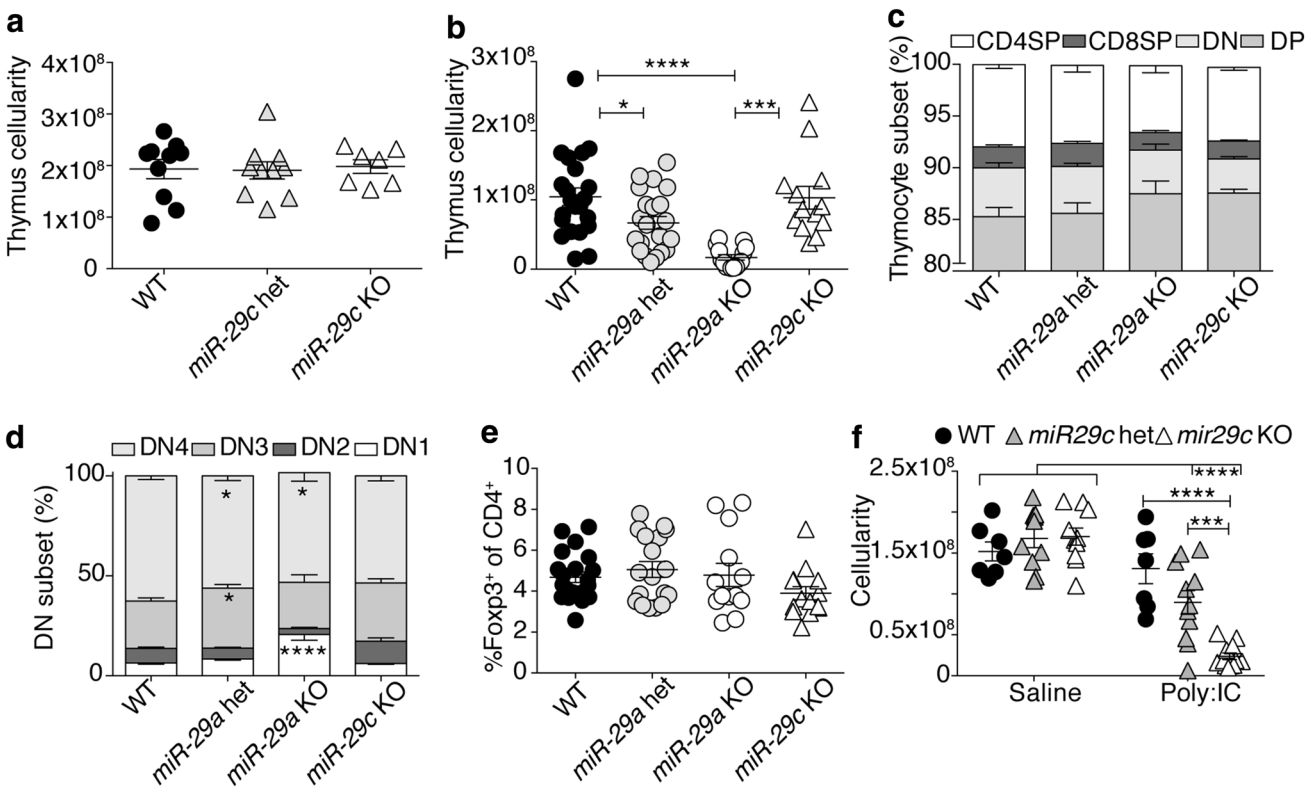

Fig. 1 Increased sensitivity to Poly(I:C)-induced thymic involution in miR-29c-deficient mice. Thymi from wild-type (WT), *miR-29a* het, *miR-29a* KO, and *miR-29c* KO mice were analyzed by flow cytometry in naïve mice (**a**–**e**) and in response to poly(I:C) treatment (**f**). **a** Thymic cellularity, 9-week-old mice ($n=10,10,7$) and **b** 20–32-week-old mice. ($n=23, 22, 15, 13$). **c** At 20–32 weeks of age, major thymic subsets, ($n=27, 20, 8, 17$) and **d** $B220^-$, double negative (DN) ($CD3^-CD4^-CD8^-$) subpopulations ($n=27, 19, 14, 17$). **e** $Foxp3^+$ cells as percentage of $CD4^+$ single positive (SP) lymphocytes ($n=21, 18, 13, 6, 14$). **f** Poly(I:C)-induced thymic involution in WT, *miR-29c* het and *miR-29c* KO mice ($n=7, 10, 10, 7, 11, 12$). Mean ± SEM, $*p<0.05$, $***p\leq0.001$, $****p\leq0.0001$

Introduction

MicroRNA (miR) are small non-coding RNAs that function as transcriptional modifiers by directly binding to mRNA target sequences, thereby destabilizing the mRNA and inhibiting protein synthesis [1]. Crucial roles in safeguarding the tolerogenic balance in the adaptive immune system, and thereby preventing autoimmunity, have been demonstrated for a number of different microRNAs, such as *miR-146a, miR-17-92, miR-21, miR-155*, and *let-7a* [2–6]; however, additional miR with functional roles in autoimmunity are likely to be identified.

The *miR-29* family (*miR-29a, miR-29b-1, miR-29b-2*, and *miR-29c*) is a family of miR expressed in two genomic clusters: the *miR-29a* cluster (*miR-29a/b-1*) and the *miR-29c* cluster (*miR-29b-2/c*) [7]. Multiple immunological functions have been reported for the *miR-29* family, including protective functions in age-related and infection-induced thymic involution [8], roles in T-cell differentiation, and inhibition of Th1 responses via suppression of T-bet, Eomes, and IFNγ mRNA [9–11] and lymphoid oncogenesis [12, 13], and a contribution to chronic inflammation in multiple sclerosis [11]. The role of the *miR-29* family in B cells has been much less studied, with the exception of oncogenic transformation, where miR-29a over-expression promotes leukemia [12].

While multiple immunological functions of the *miR-29* family have been defined, relatively little is known about the individual roles of the each cluster, with studies focusing on a single *miR-29* family member or using pan-*miR-29* blockade. While the seed sequences of each family member are identical, differing expression patterns and non-seed sequences can drive distinct functions for each family member, as recently characterized in the endocrinological context [14]. Here, we study the role of the individual clusters of the *miR-29* family (*miR-29a/b-1* and *miR-29b-2/c*) in T-cell development and collagen-induced arthritis (CIA). We find a subservient role for *miR-29c* in T-cell development, and a protective hierarchy of function in the CIA model, with *miR-29a* being dominant, revealing a critical function in the B-cell germinal center response.

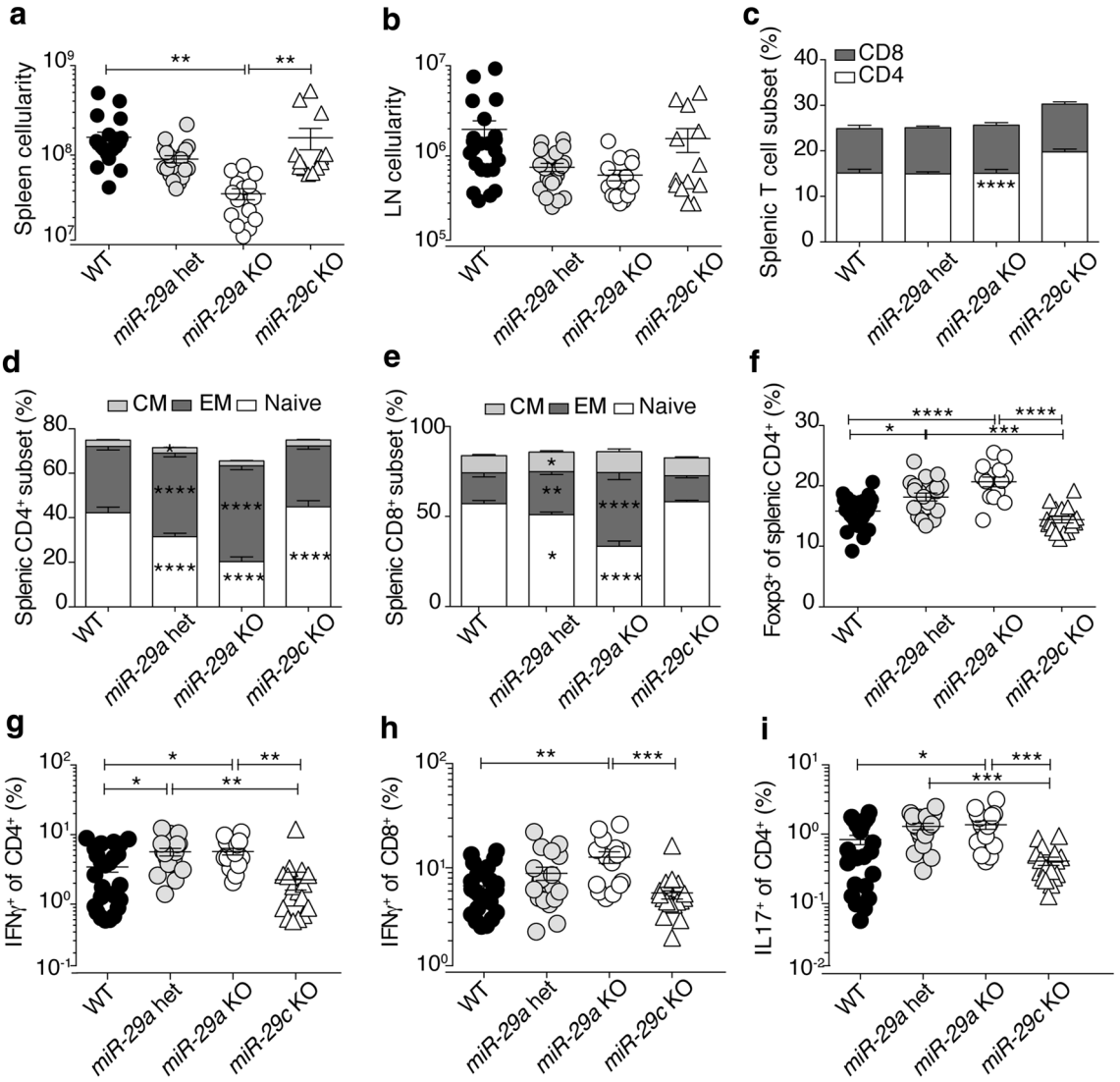

Fig. 2 Composition of T-cell subsets in the peripheral lymphoid organs is not dependent on miR-29b-2/c. T-cell subsets in spleen and superficial LN of 20–32-week-old naïve WT, *miR-29a* het, *miR-29a* KO, and *miR-29c* KO mice were analyzed by flow cytometry. **a** Spleen and **b** lymph node cellularity ($n=23$, 22, 15, 9, 13). **c** Percentage of $CD4^+$ and $CD8^+$ T cells in the spleen. **d** Naïve, EM, and CM T cells within $CD4^+$ and **e** $CD8^+$ T cells in the spleen. **f** $Foxp3^+$ regulatory T cells as a percentage of $CD4^+$ T cells in the spleen ($n=27$, 20, 14, 17). **g** IFNγ production by $CD4^+$ and **h** $CD8^+$ T cells after stimulation *in vitro*, and **i** IL-17 production by $CD4^+$ T cells after stimulation *in vitro* ($n=26$, 18, 16, 17). Mean ± SEM. $^*p<0.05$, $^{**}p\leq0.01$, $^{***}p\leq0.001$, $^{****}p\leq0.0001$ compared to WT

Materials and methods

Mice

miR-29a/b-1 (*miR-29a*) and *miR-29b-2/c* (*miR-29c*) knockout mice were described previously [8, 14]. For thymic involution, suboptimal doses of 150 µg/mouse Poly(I:C) (Invivogen, CA, USA) [8], or control saline, were injected intraperitoneally on days 0 and 2, with thymic cellularity determined on day 3. Control mice received saline injections. To determine the germinal center response, mice (8–12 wks) were immunized i.p. with 2×10^9 SRBCs. Spleens were analyzed by flow cytometry 8 days after immunization.

Flow cytometry

Surface staining was performed in RPMI containing 2% fetal bovine serum and anti-mouse CD16/CD32 antibodies (from hybridoma supernatant generated in-house). The following antibodies were used in this study: CD11c (N418) (Biolegend), CD138 (281-2) and CD64 (X54-5/7.1.1), (BD-Pharmingen), and B220 (RA3-6B2), CD19 (eBio1D3), CD3 (145-2C11), CD4 (GK1.5 and

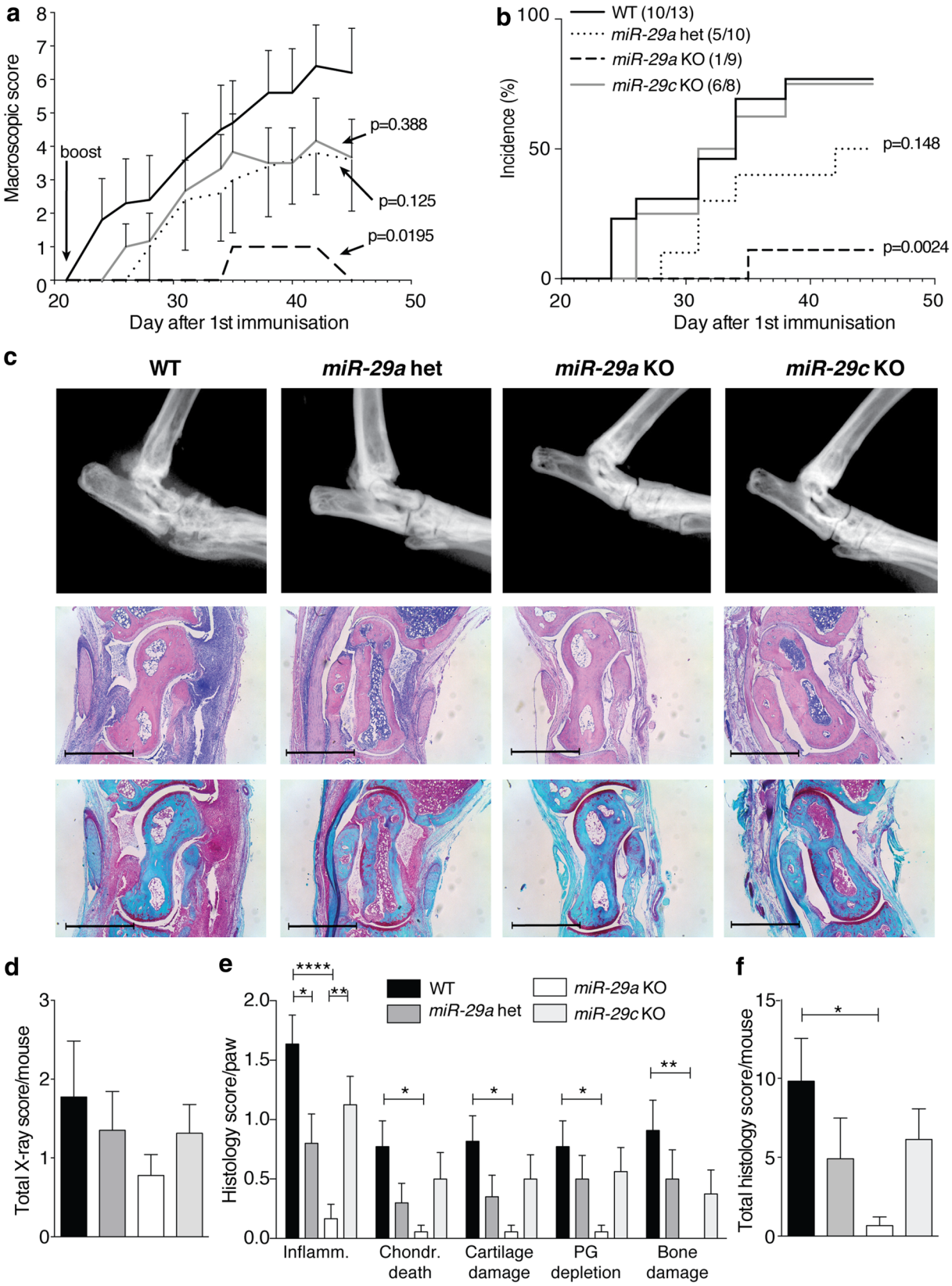
a
Macroscopic score
boost
p=0.388
p=0.125
p=0.0195
Day after 1st immunisation
b
WT (10/13)
miR-29a het (5/10)
miR-29a KO (1/9)
miR-29c KO (6/8)
Incidence (%)
p=0.148
p=0.0024
Day after 1st immunisation
c
WT
miR-29a het
miR-29a KO
miR-29c KO
d
Total X-ray score/mouse
e
WT
miR-29a het
miR-29a KO
miR-29c KO
Histology score/paw
Inflamm.
Chondr. death
Cartilage damage
PG depletion
Bone damage
f
Total histology score/mouse

◂**Fig. 3** Loss of miR-29 protects from autoimmune pathology in collagen-induced arthritis. Collagen-induced arthritis (CIA) was induced in 12–14 week old WT, *miR-29a* het, *miR-29a* KO, and *miR-29c* KO mice. Arthritis was scored three times weekly until sacrifice on day 45, when serum and paws were taken for downstream analysis. **a** Macroscopic score of paws (arthritic mice shown only, cumulative scores of 0–3 per paw, $n=13$, 10, 9, 8). **b** Incidence of arthritis for each genotype. **c** Representative photos of X-ray analysis, H&E stain, and Safranin O stain of the ankle joints for each group. Scale bar = 1 mm. **d** Pooled X-ray scores of for each group (maximum score per mouse = 8, $n=11$, 10, 9, 8). **e** Detailed histological scores of the ankle joints (maximum score per feature = 3, $n=22$, 20, 18, 16 joints per group). **f** Total histological scores per mouse ($n=11$, 10, 9, 8). Mean ± SEM. $^{*}p<0.05$, $^{**}p\leq0.01$, $^{****}p\leq0.0001$

RM4-5), CD95 (15A7), CXCR5 (SPRCL5), CD44 (IM7), CD62L (MEL-14), CD8α (53–6.7) FoxP3 (FJK-16s), IFNγ (XMG1.2), IgM (eB121-15F9 and II/41), IgD (11-26c), IL-17 (TC11-18H10), IL-4 (BVD6-24G2), PD-1 (J43), GL-7 (GL7), CD43 (eBioR2/60), Gr1 (RB6-8C5), CD11b (M1/70), CD86 (PO3.1), CD24 (M1/69), CD23 (B3B4), CD80 (16-10A1), CD21 (eBio8D9), MHCII (M5/114.15.2), Ly6C (HK1.4), PDCA-1 (eBio927), and CD31 (390) (eBioscience, CA, USA). Nuclear staining for Foxp3 was performed using the Foxp3 staining kit (eBioScience, CA, USA). Cytoplasmic intracellular staining for cytokines was performed following a 4-h stimulation with 50-ng/mL phorbol 12-myristate 13-acetate and 0.5-µg/mL ionomycin in the presence of GolgiStop (Monensin A, BD Biosciences, NJ, USA) using the Cytofix/Cytoperm kit (BD Biosciences, NJ, USA). Dead cell exclusion stain was performed using Zombie dyes (BioLegend, San Diego, CA, USA) according to the manufacturer's instructions. Flow cytometric data were collected on a BD FACSCanto II Flow Cytometer (BD Biosciences) and analyzed using the FlowJo software (Treestar Inc., OR, USA).

Collagen-induced arthritis

CIA was induced as described in 6–10-week-old mice [15]. A total of 100 µL of chick type II collagen (CII, final concentration 1 mg/ml; Sigma, MO, USA) emulsified in complete Freund's adjuvant containing 5-mg/ml heat-killed *M. tuberculosis* H37RA (BD Difco, NJ, USA) was injected intradermally in two sites at the base of the tail. The injection was repeated 21 days later. Animals were monitored every 2 days for erythema and swelling of limbs, and a clinical score (0–3) was given for each paw. At sacrifice, paws were taken and fixed in 4% neutral buffered paraformaldehyde solution and processed for X-ray analysis (Faxitron MX20 instrument, Faxitron Bioptics, AZ, USA) and histology. Serum was collected using serum tubes (Greiner, Vilvoorde, Belgium) and analyzed for anti-collagen antibodies, rheumatoid factor (RF), and IFNγ by ELISA.

Serum analysis

Serum IFNγ (eBioscience, CA, USA) was measured by ELISA according to the manufacturer's recommendations. The anti-chick collagen II IgG ELISA was performed as described [16]. Rabbit-anti-mouse IgG coupled to horseradish peroxidase (HRP, Southern Biotech, IL, USA) was used as detection antibody. Standard curves were constructed from pooled sera of CII hyper-immunized DBA/1 mice, set at 100,000 units/mL.

Histology

Joints were fixed in 4% neutral buffered paraformaldehyde, decalcified in 5% formic acid, and embedded in paraffin. 7-µM sections were cut and stained with haematoxylin and eosin (H&E, Polysciences, PA, USA) or Safranin O (SafO, Sigma, MO, USA) according to the manufacturer's recommendations. Inflammation, chondrocyte death, bone destruction, cartilage damage, and proteoglycan (PG) depletion were scored on a scale of 0–3 per feature by a researcher blinded to the experimental groups.

B- and T-cell stimulation in vitro

Total splenocytes were labeled with CFSE (0.25 µM; Molecular Probes) and plated in a 96-well plate at the concentration of 0.25×10^6 cells/well/100 µl for 4 days with the following stimulation: media alone, goat anti-mouse IgM $F(ab)_2$ (20 µg/mL; Jackson Immunoresearch), LPS (10 µg/mL; Sigma-Aldrich), or phorbol myristate acetate (PMA, 50 ng/mL; Sigma-Aldrich) and ionomycin (250 ng/mL; Sigma-Aldrich). Cells were stained and analyzed by flow cytometry on day 4 as described above. Division index was defined as the average number of cell divisions.

Statistical analysis

Statistical significance was determined using the GraphPad Prism 6 software package (GraphPad software, CA, USA). Regular one-way or two-way ANOVA was used followed by Tukey's or Sidak's multiple comparisons tests to compare the different groups. Where only two groups were analyzed, the Mann–Whitney test was used. For statistical analysis of arthritis severity, the area under the curve for each individual mouse was determined, and compared to WT using two-way ANOVA. Significance for arthritis incidence was determined by survival curve analysis. *P* values < 0.05 were considered significant.

Results

Deficiency in miR-29c sensitizes the thymus for inappropriate involution

Our earlier studies showed that mice deficient for thymic expression of *miR-29a/b-1* display aberrant thymic involution at an early age [8]. As *miR-29b-2/c* is also expressed in the thymic epithelium and has an identical seed sequence [8], we sought to determine whether spontaneous thymic involution was also observed following deficiency in the *miR-29c* locus. Naïve wild-type mice (WT), *miR-29b-2/c* heterozygous (*miR-29c* het), and *miR-29b-2/c* knockout (*miR-29c* KO) mice were assessed for thymic cellularity and T-cell populations at 9 weeks and at 20–23 weeks of age (Fig. 1a, b). Unlike mice deficient for the *miR-29a/b-1* cluster (*miR-29a* KO mice) [8], the thymic cellularity of *miR-29c* KO mice was comparable to WT mice at both ages, with no sign of spontaneous involution. Notably, *miR-29a* heterozygous (*miR-29a* het) mice showed a partial phenotype, with reduced thymic cellularity in aged mice (Fig. 1b). Likewise, *miR-29c* KO mice showed no changes in the percentages of double negative (DN), double positive (DP), CD4 single positive (CD4SP), or CD8 single positive (CD8SP) cells (Fig. 1c), in DN subpopulations DN1-DN4 (Fig. 1d), or thymic Foxp3$^+$CD4$^+$ regulatory T cells (Treg, Fig. 1e). These results indicate that *miR-29c* is less important in thymic function than *miR-29a*, with no apparent spontaneous phenotype in the knockout.

miR-29a KO mice not only display spontaneous thymic involution, but are also hypersensitive to poly(I:C)-induced thymic involution [8]. Poly(I:C) injection reproduces the effect of pathogen-associated molecular pattern (PAMP) exposure, such as occurs during viral infection, leading to thymic involution [17]. While *miR-29c* KO mice did not show spontaneous thymic involution (Fig. 1b), we sought to determine whether a function of *miR-29c* would be revealed through challenging the thymus. To detect hypersensitivity, we injected suboptimal doses of poly(I:C) in the *miR-29c* KO mice, at a level which did not induce thymic involution in WT mice (Fig. 1f). Both *miR-29c* KO mice, and, to a lesser extent, *miR-29c* het mice exhibited thymic involution after challenge with suboptimal poly(I:C) levels. These results suggest a distinct hierarchy of importance for *miR-29* family members in thymic involution, with *miR-29a* playing the dominant role in preventing inappropriate thymic involution (with both knockout and heterozygous presenting with spontaneous involution), while *miR-29c* has a subservient, but measurable, function, only revealed using sensitized screens.

miR-29a is the dominant miR-29 family member in peripheral lymphocytes

As the relative expression of *miR-29* family members can vary during differentiation, we sought to extend the hierarchical comparison from the thymus to the periphery. Spleen and superficial lymph nodes (LN) of 20–32 week-old naïve WT, *miR-29a* het, *miR-29a* KO, *miR-29c* het and *miR-29c* KO mice were analyzed by flow cytometry to compare the function of *miR-29* family members in peripheral lymphocyte populations. Splenic and lymph node cellularity which were twofold reduced in *miR-29a* KO mice, however, did not differ in *miR-29c* het or KO mice (Fig. 2a, b). In *miR-29a* KO mice, the number of CD4$^+$ and CD8$^+$ T cells in the spleen was not disturbed (Fig. 2c), but the relative contribution of effector-memory cells was increased at the expense of naïve cells (Fig. 2d, e), and the number of Foxp3$^+$ Tregs was increased (Fig. 2f). As with the thymic phenotype, intermediate phenotypes were observed in heterozygous mice. By contrast, these changes were not observed in *miR-29c* KO mice (Fig. 2d–f). Similar effects were observed with cytokine production, with *miR-29a*-deficient mice having increased IFNγ and IL-17 production, while *miR-29c*-deficient mice remained normal (Fig. 2g–i). Together, these results indicate that the importance of the *miR-29* family observed in peripheral T cells can be largely, if not exclusively, attributed to *miR-29a*, with no spontaneous phenotype observed with *miR-29c* deficiency.

A hierarchical role for the miR-29 family in autoimmune disease

Analysis of the immune system under homeostatic conditions identified *miR-29a* as having multiple potent functions, while deficiency in *miR-29c*, despite the identical seed sequence between the two family members, had no impact. However, these results do not preclude a more subtle phenotype from being revealed upon immunological challenge, such as during autoimmunity. We, therefore, sought to identify the roles of miR-29 family members in autoimmunity, using the model of CIA. Arthritis was induced by collagen immunization in WT, *miR-29a* het, *miR-29a* KO, and *miR-29c* KO mice. Mice were monitored for 45 days through macroscopic inspection of the paws 3 times weekly. Surprisingly, *miR-29a* KO mice were almost completely protected from CIA, with both the severity and incidence of CIA markedly reduced. Only 1 (out of 9) of the *miR-29a* KO mice was affected, and the pathology in this mouse was transient and limited to 1 digit (Fig. 3a, b). The *miR-29a* het and *miR-29c* KO mice displayed a reduction in severity, albeit not statistically different from the WT mice.

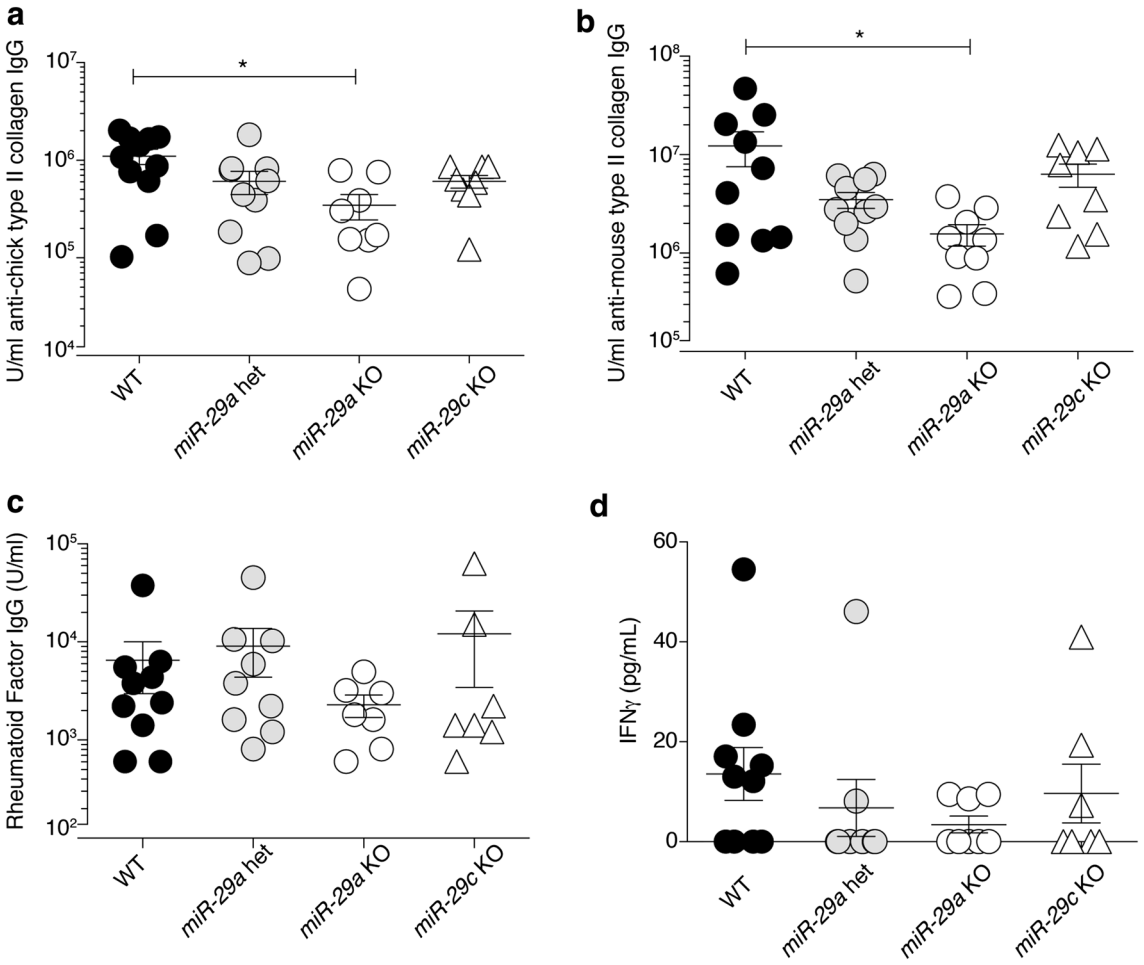

Fig. 4 Reduced anti-collagen response in *miR-29a* KO mice after collagen-induced arthritis. **a** Serum levels of anti-chick collagen type II, **b** anti-mouse collagen type II, **c** rheumatoid factor (RF) ($n=10$, 10, 9, 8), and **d** IFNγ ($n=10$, 8, 8, 7) were determined by ELISA. Mean ± SEM. *$p<0.05$

The resistance to CIA observed in *miR-29a*-deficient mice at the macroscopic level was also observed at the anatomical and histological levels. Ankle joints were visualized by X-ray to determine the extent of bone damage and joint morphology. Damage was apparent in the small joints of the ankle and foot of the WT mice, while very little damage was apparent in *miR-29a* KO mice (Fig. 3c). Again, an intermediate phenotype was observed for *miR-29a* het and *miR-29c* KO mice, although the pooled X-ray scores were not significantly different between groups (Fig. 3d). Additional features of joint pathology were scored on H&E and SafO stained paraffin sections of the large ankle joints. For all features scored (inflammation, chondrocyte death, cartilage damage, proteoglycan depletion, and bone damage), *miR-29a* KO mice had significantly less severe lesions, or complete absence of pathology (Fig. 3c, e). *miR-29a* het and *miR-29c* KO mice also had reduced pathology for all features scored, although only the inflammatory infiltrate in the *miR-29a* het mice was significantly different from the WT. These results were reflected in the overall histological scores (Fig. 3f). Reduced pathology in *miR-29a*-deficient mice was accompanied by a poor antibody response to the immunization with collagen, as measured by serum antibody levels of anti-chick and anti-mouse type II collagen (CII) antibodies (Fig. 4a, b), while rheumatoid factor (RF) remained normal (Fig. 4c). Despite increased production of IFNγ by *miR-29a* KO $CD4^+$ and $CD8^+$ T cells (Fig. 2g, h), IFNγ levels in the serum were not increased during CIA (Fig. 4d), and therefore, protection against CIA cannot be explained by over-expression of IFNγ [18, 19]. Together, these results suggest that *miR-29a* is essential to suppress inflammatory cytokines, but also to mount an appropriate immunization response. In contrast, *miR-29c* only had minor or no effects on these biological processes, despite being expressed in the same cell types and sharing the seed sequence with *miR-29a*.

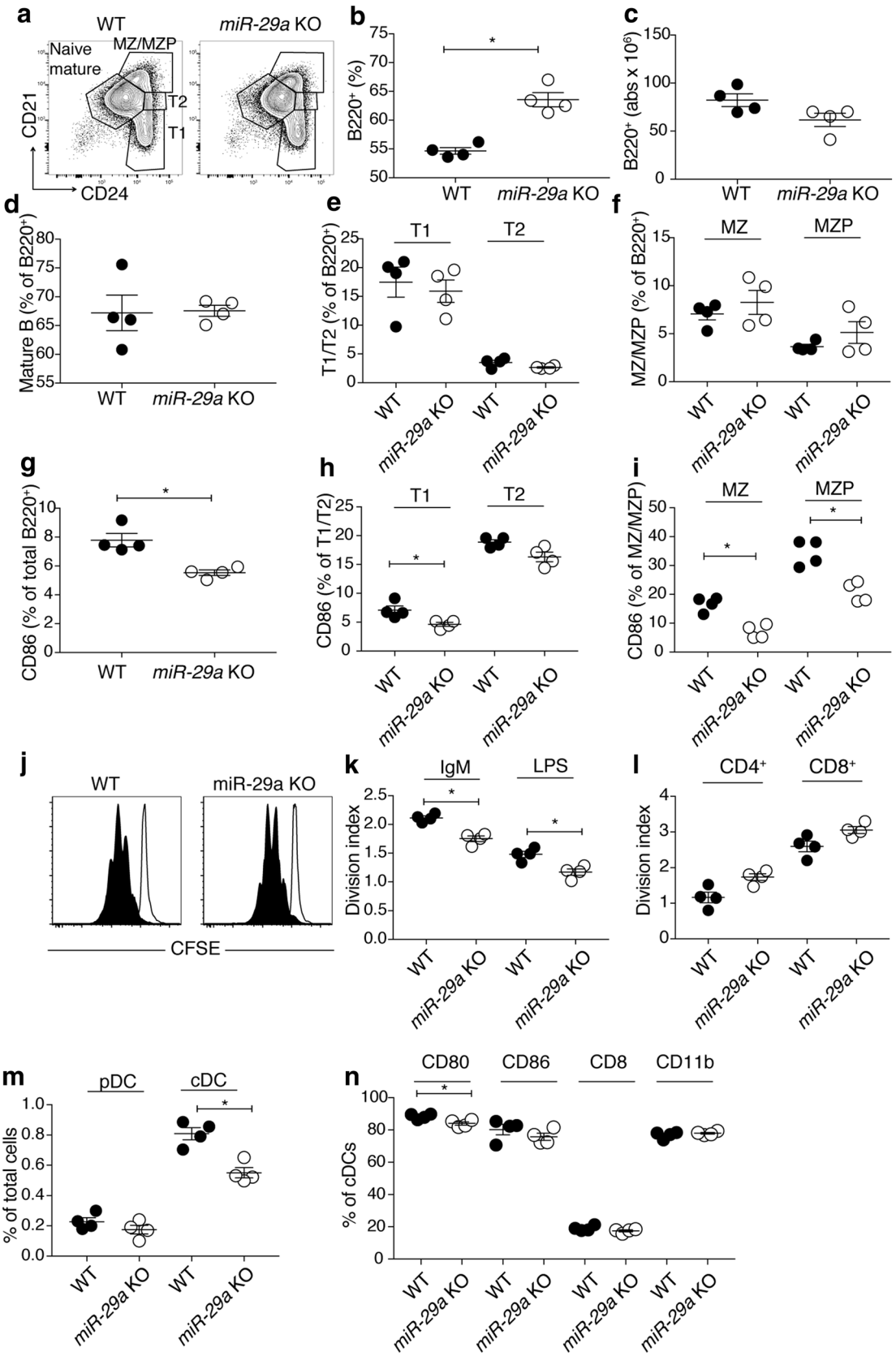
a
WT
miR-29a KO
Naive mature
MZ/MZP
T2
T1
CD21
CD24
b
B220+ (%)
WT
miR-29a KO
c
B220+ (abs x 10^6)
WT
miR-29a KO
d
Mature B (% of B220+)
WT
miR-29a KO
e
T1
T2
T1/T2 (% of B220+)
WT
miR-29a KO
f
MZ
MZP
MZ/MZP (% of B220+)
WT
miR-29a KO
g
CD86 (% of total B220+)
WT
miR-29a KO
h
T1
T2
CD86 (% of T1/T2)
WT
miR-29a KO
i
MZ
MZP
CD86 (% of MZ/MZP)
WT
miR-29a KO
j
WT
miR-29a KO
CFSE
k
IgM
LPS
Division index
WT
miR-29a KO
l
CD4+
CD8+
Division index
WT
miR-29a KO
m
pDC
cDC
% of total cells
WT
miR-29a KO
n
CD80
CD86
CD8
CD11b
% of cDCs
WT
miR-29a KO

◂**Fig. 5** Altered B-cell numbers and activation and reduced DC activation in *miR-29a* KO mice. Spleens from 6- to 12-week-old naïve WT and *miR-29a* KO mice (4,4) were analyzed either directly *ex-vivo* (a–i, m,n) or after stimulation with IgM or LPS *in vitro* (j–l) by flowcytometry for B-cell and DC subsets and activation markers. **a** Gating strategy for B-cell populations, **b** percentage $B220^+$ cells of total splenocytes, **c** absolute number of $B220^+$ cells in the spleen, **d–f** B-cell subsets mature, transitional ½, and marginal zone/marginal zone progenitors as % of total $B220^+$ cells, and **g–i** expression of CD86 on B-cell subsets. **j–l** Splenocytes were labeled with CFSE and B cells were assessed for proliferation after 4 days of culture. **j** Representative CFSE histograms of B cells from WT and *miR-29a* KO mice after stimulation with IgM (filled histograms) or media alone (clear histograms), **k** division index of B cells after 4 days of IgM or LPS stimulation, **l** division index of $CD4^+$ and $CD8^+$ T cells after 3-day stimulation with PMA/ionomycin, **m** pDC and cDC populations in the spleen, and **n** surface markers of splenic cDC. Mean ± SEM. $*p < 0.05$

Reduced production of germinal center B cells in miR-29a KO mice

The resistance against arthritis development in the *miR-29a* KO mice may be a direct result of a reduced immunization response caused by altered B-cell populations or activation. We analyzed the B-cell compartment in the bone marrow (BM), and analyzed both the B-cell compartment and DC populations in the spleens of naïve *miR-29a* KO mice (Fig. 5). In the BM, we found no difference in B-cell numbers or populations (data not shown). However, although the percentage of B cells in the spleen of naïve *miR-29a* KO mice was increased (Fig. 5b), the absolute number of B cells was within the normal range (Fig. 5c). There was no difference in the B-cell subsets mature (M), transitional (T1 and T2), marginal zone (MZ), and marginal zone progenitors (MZP) between the WT and *miR-29a* KO mice (Fig. 5d–f); however, the expression of co-stimulatory molecule CD86 on total B cells, T1/T2, and MZ/MZP was markedly reduced in the *miR-29a* KO mice, indicative of reduced activation (Fig. 5g–i). An intrinsic defect in *miR-29a* KO B cells in response to stimulation was confirmed *in vitro* by stimulation of B cells using IgM and LPS (Fig. 5j, k). Fewer *miR-29a* KO B cells divided upon stimulation, and those that divided reached a lower number of divisions after 4 days compared to the WT B cells (Fig. 5k). In contrast, this defect was not observed in T cells stimulated with PMA/ionomycin in the same assay (Fig. 5l). As the immunization response also involves DC, we analyzed different DC populations in the spleen of naïve *miR-29a* KO mice (Fig. 5m, n). We found reduced conventional DC (cDC, Fig. 5m), and in addition a minor reduction of $CD80^+$ cDC (Fig. 5n). These data indicate that, indeed, the *miR-29a* KO B cells are impaired in activation and proliferation *in vitro*.

To directly evaluate germinal center populations *in vivo*, we analyzed the B- and T-cell populations in the spleen after immunization with sheep red blood cells (SRBC, Fig. 6a–c). Following the immunization, *miR-29a* KO mice had normal $CD4^+$ T-cell responses (Fig. 6d), but with an over-representation of $Foxp3^+$ Treg (Fig. 6e), as previously shown for unimmunized mice (Fig. 2). The T-cell response of *miR-29a* KO mice to immunization was within the normal range, with normal production of follicular helper T cells (Tfh) (Fig. 6f), coupled with a non-significant increase in follicular regulatory T cells (Tfr), paralleling the increased Treg number (Fig. 6g). Despite the normal follicular T-cell response, germinal center B-cell (GCB) formation was sharply impaired (Fig. 6h), although plasmablasts were not significantly altered (Fig. 6i). Together, these results indicate that miR-29a KO mice have an innate defect in B-cell activation and germinal center production. In the context of an arthritic response, this B-cell defect may account for the reduced autoantibody production and autoimmune pathology manifested by KO mice.

Discussion

The high expression of *miR-29* family members in the immune system and the relative enrichment of immunological genes among predicted targets [7] have led to a detailed search for immunological function. The key functions identified for the *miR-29* family in the immune system include preservation of thymic tissue during development [8], restraining polarization of T cells towards the Th1 lineage [9] and promoting B-cell oncogenesis [12]. However, these studies have mostly relied on research tools that either specifically target the *miR-29a/b-1* cluster [8, 12, 20] or do not differentiate between family members (such as expression of a *miR-29* "sponge" [10] or reconstitution studies which negate the differentiation expression patterns [9]). This research design has led to a paucity of information about the relative contribution of the *miR-29b-2/c* cluster on these same immunological processes.

In this study, by directly comparing deficiency in the two *miR-29* clusters, we were able to establish a distinct functional hierarchy. For the known functions of *miR-29a* in T-cell biology, the functional consequences of *miR-29c*-deficiency were minor or not detected. Thus, no spontaneous thymic involution was observed for *miR-29c*-deficient mice, and no elevation of Th1 polarization was detected in the periphery. However, there were indications that the same biological processes are controlled by both *miR-29a* and *miR-29c*, as the *miR-29c* KO mice were sensitive to developing parallel phenotypes upon induction, even if they did not exhibit them spontaneously under homeostatic conditions. These studies even allow a rough baseline of the relative importance of *miR-29a* and *miR-29c* clusters to be estimated, as the *miR-29c* KO was similar, or slightly weaker, than the *miR-29a*

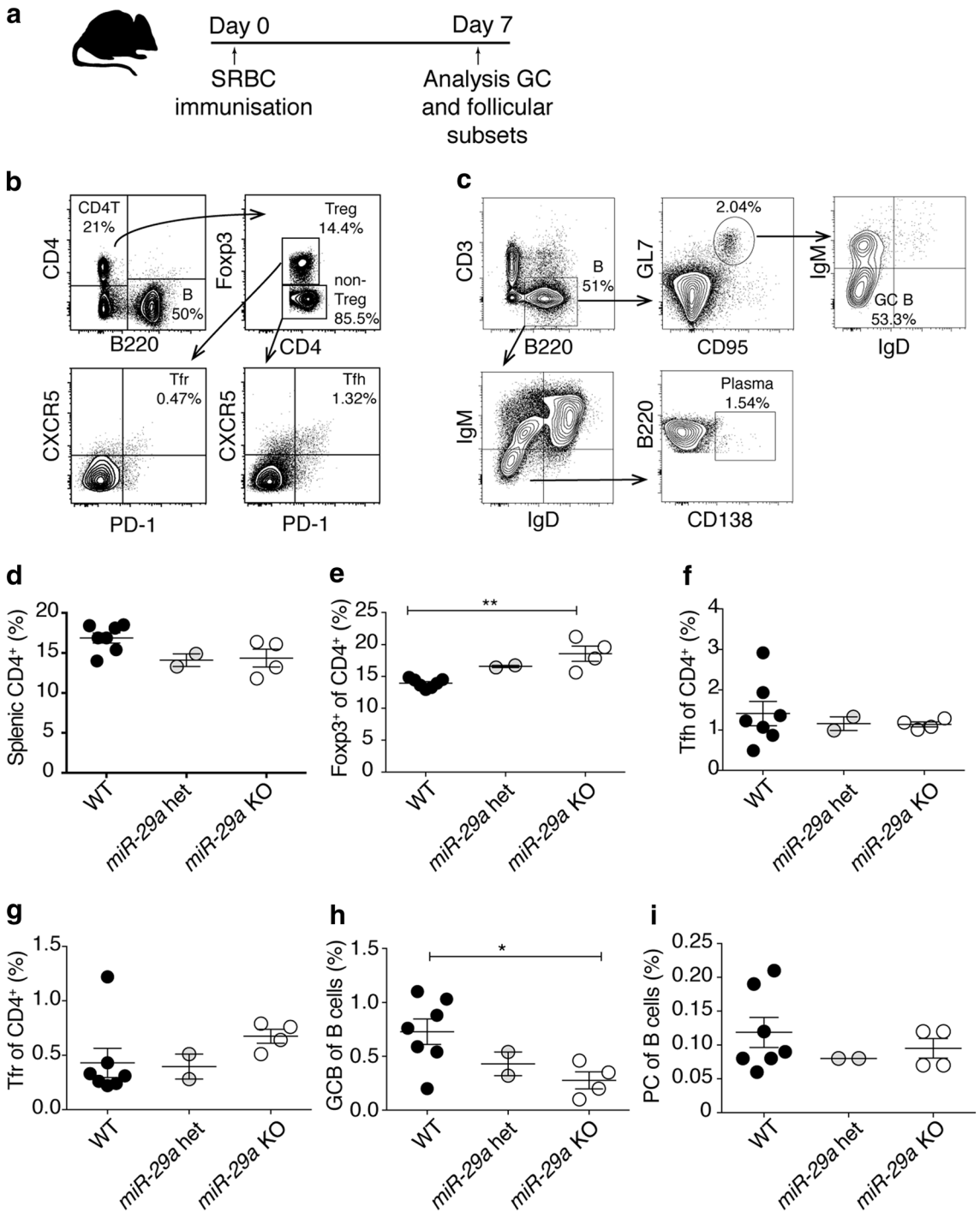

Fig. 6 Loss of miR-29a leads to a reduction in germinal center B cells. 6–12-week-old WT, *miR-29a* het and *miR-29a* KO mice ($n=7$, 2, 4) were immunized with SRBC, and 8 days later, cell populations in the spleen were analyzed by flow cytometry. **a** Immunization strategy, and **b** gating strategy for Tfh and Tfr and **c** GC B cells and plasma cells. **d** Splenic $CD4^+$ T cells, **e** splenic $Foxp3^+$ Treg, **f** Tfh, **g** Tfr, **i** GCB, and **h** plasmablasts 8 days after immunization. Mean ± SEM. $*p<0.05$, $**p\leq0.01$

heterozygous mouse. Intriguingly, this same hierarchy and relative importance were observed in a recent analysis of *miR-29a* and *miR-29c* clusters in glucose handling [14], despite the processes being controlled by different molecular circuits in different organs. It is tempting to speculate that *miR-29a* is the primary cluster of the *miR-29* family, with *miR-29c* existing only to boost overall expression levels to avoid the early lethality of complete

miR-29 deficiency [14]; however, it is also possible that the hierarchy observed in the immune and endocrine systems may be inverted in other tissues or processes.

The protective effect of *miR-29a*-deficiency on CIA is counter-intuitive when considering the pro-inflammatory impact, this deficiency has on T cells [9]. A complementary result was observed in Experimental Autoimmune Encephalomyelitis, the mouse model of Multiple Sclerosis [11], which together suggests that *miR-29a*-deficient T cells, while showing enhanced polarization towards inflammatory lineages, are incapable of promoting effective pathogenic reactions. However, as with other miR, it needs to be considered that *miR-29a* has a broad expression beyond T cells, and the CIA model is driven by a complex interaction of multiple cell types. Both T cells and B cells are important for disease development, and the local tissue and resident immune cells also shape the nature of the response [15]. Mechanistic dissection of the B-cell compartment led to observations compatible with this model; namely defects in B-cell proliferation, germinal center differentiation, and antibody production.

Thus, it is possible that the function of *miR-29a* is pro-pathogenic in the T-cell context, but strongly anti-pathogenic in the B-cell context, leading to a net effect of a global knockout of *miR-29a* which is anti-pathogenic. We note, however, that the arthritic reaction is highly complex, and a role for other cell types cannot be excluded at this stage, including the potential for defective costimulation by B cells and DCs. In this regard, assessment of the arthritic potential of *miR-29a* using other models (such as B-cell-specific over-expression of *miR-29a* [12], or using T-cell transfer models with wild-type T cells into *miR-29a*-deficient hosts) may shed light on the potential utility of *miR-29a* inhibition as an anti-arthritic treatment.

Acknowledgements The authors wish to thank Josselyn E. Garcia-Perez, Denise Klatt, Birgitte Walgreen, Monique Helsen, and Alessio Zuppelli for help with experiments, Susann Schönefeldt and Jeason Haughton for help with mouse breeding, and the Leuven University Animalium staff for animal husbandry. This work was supported by the Flemish Institute for Biotechnology (VIB), the Belgian Science Policy Office Interuniversity Attraction Poles program (T-TIME) and the Fonds Wetenschappelijk Onderzoek (FWO) Flanders. AvN was supported by the Leuven University F+fellowship, SMS and SH-B were supported by FWO fellowships.

Compliance with ethical standards

Ethical standards All experiments were approved by the Animal Ethics Committee of the University of Leuven.

Conflict of interest The authors declare that they have no conflict of interest.

References

1. Ambros V (2004) The functions of animal microRNAs. Nature 431:350–355
2. Boldin MP, Taganov KD, Rao DS, Yang L, Zhao JL, Kalwani M, Garcia-Flores Y, Luong M, Devrekanli A, Xu J, Sun G, Tay J, Linsley PS, Baltimore D (2011) miR-146a is a significant brake on autoimmunity, myeloproliferation, and cancer in mice. J Exp Med 208:1189–1201
3. Xiao C, Srinivasan L, Calado DP, Patterson HC, Zhang B, Wang J, Henderson JM, Kutok JL, Rajewsky K (2008) Lymphoproliferative disease and autoimmunity in mice with increased miR-17-92 expression in lymphocytes. Nat Immunol 9:405–414
4. Garchow B, Kiriakidou M (2016) MicroRNA-21 deficiency protects from lupus-like autoimmunity in the chronic graft-versus-host disease model of systemic lupus erythematosus. Clin Immunol 162:100–106
5. Kurowska-Stolarska M, Alivernini S, Ballantine LE, Asquith DL, Millar NL, Gilchrist DS, Reilly J, Ierna M, Fraser AR, Stolarski B, McSharry C, Hueber AJ, Baxter D, Hunter J, Gay S, Liew FY, McInnes IB (2011) MicroRNA-155 as a proinflammatory regulator in clinical and experimental arthritis. Proc Natl Acad Sci USA 108:11193–11198
6. Guan H, Fan D, Mrelashvili D, Hao H, Singh NP, Singh UP, Nagarkatti PS, Nagarkatti M (2013) MicroRNA let-7e is associated with the pathogenesis of experimental autoimmune encephalomyelitis. Eur J Immunol 43:104–114
7. Liston A, Papadopoulou AS, Danso-Abeam D, Dooley J (2012) MicroRNA-29 in the adaptive immune system: setting the threshold. Cell Mol Life Sci 69:3533–3541
8. Papadopoulou AS, Dooley J, Linterman MA, Pierson W, Ucar O, Kyewski B, Zuklys S, Hollander GA, Matthys P, gray DHD, De Strooper B, Liston A (2012) The thymic epithelial microRNA network elevates the threshold for infection-associated thymic involution via miR-29a mediated suppression of the IFN-α receptor. Nat Immunol 13:181–187
9. Steiner DF, Thomas MF, Hu JK, Yang Z, Babiarz JE, Allen CDC, Matloubian M, Blelloch R, Ansel KM (2011) MicroRNA-29 regulates T-box transcription factors and interferon-γ production in helper T cells. Immunity 35:169–181
10. Ma F, Xu S, Liu X, Zhang Q, Xu X, Liu M, Hua M, Li N, Yao H, Cao X (2011) The microRNA miR-29 controls innate and adaptive immune responses to intracellular bacterial infection by targeting interferon-γ. Nat Immunol 12:861–869
11. Smith KM, Guerau-de-Arellano M, Costinean S, Williams JL, Bottoni A, Mavrikis Cox G, Satoskar AR, Croce CM, Racke MK, Lovett-Racke AE, Whitacre CC (2012) miR-29ab1 deficiency identifies a negative feedback loop controlling Th1 bias that is dysregulated in multiple sclerosis. J Immunol 189:1567–1576
12. Santanam U, Zanesi N, Efanov A, Costinean S, Palamarchuk A, Hagan JP, Volinia S, Alder H, Rassenti L, Kipps T, Croce CM, Pekarsky Y (2010) Chronic lymphocytic leukemia modeled in mouse by targeted miR-29 expression. Proc Natl Acad Sci USA 107:12210–12215
13. Kincaid RP, Burke JM, Sullivan CS (2012) RNA virus microRNA that mimics a B-cell oncomiR. Proc Natl Acad Sci USA 109:3077–3082
14. Dooley J, Garcia-Perez JE, Sreenivasan J, Schlenner SM, Vangoitsenhoven R, Papadopoulou AS, Tian L, Schonefeldt S, Serneels L, Deroose C, Staats KA, Van der Schueren B, De Strooper B, McGuinness OP, Mathieu C, Liston A (2016) The microRNA-29 family dictates the balance between homeostatic and pathological glucose handling in diabetes and obesity. Diabetes 65:53–61

15. Campbell IK, Hamilton JA, Wicks IP (2000) Collagen-induced arthritis in C57BL/6 (H-2b) mice: new insights into an important disease model of rheumatoid arthritis. Eur J Immunol 30:1568–1575
16. Campbell IK, Rich MJ, Bischof RJ, Dunn AR, Grail D, Hamilton JA (1998) Protection from collagen-induced arthritis in granulocyte-macrophage colony-stimulating factor-deficient mice. J Immunol 161:3639–3644
17. Anz D, Thaler R, Stephan N, Waibler Z, Trauscheid MJ, Scholz C, Kalinke U, Barchet W, Endres S, Bourquin C (2009) Activation of melanoma differentiation-associated gene 5 causes rapid involution of the thymus. J Immunol 182:6044–6050
18. Kelchtermans H, Billiau A, Matthys P (2008) How interferon-gamma keeps autoimmune diseases in check. Trends Immunol 29:479–486
19. Lee J, Lee J, Park M-K, Lim M-A, Park E-M, Kim E-K, Yang E-J, Lee S-Y, Jhun J-Y, Park S-H, Kim H-Y, Cho M-L (2013) Interferon gamma suppresses collagen-induced arthritis by regulation of Th17 through the induction of indoleamine-2,3-deoxygenase. PLoS One 8:e60900
20. Braconi C, Kogure T, Valeri N, Huang N, Nuovo G, Costinean S, Negrini M, Miotto E, Croce CM, Patel T (2011) microRNA-29 can regulate expression of the long non-coding RNA gene MEG3 in hepatocellular cancer. Oncogene 30:4750–4756